

be the row-1 signalling activity during gastrulation. Although our data concur with the possibility that anterior ectodermal cells acquire their inducing properties in response to signals from the organizer, this is not certain. Signals from endoderm in anterior regions of mouse and frog embryos are required for anterior development^{16–19}, and could be involved in induction of row-1 activity. It is unknown at present which cells in zebrafish correspond to the extra-embryonic endoderm of mice or deep endodermal cells of *Xenopus*. However, the YSL shows localized inductive activity²⁰, indicating that it could be a source of signals at the anterior end of the zebrafish embryo. The possible involvement of anterior endoderm in head patterning, together with the data we present here, indicate that early patterning of anterior regions of the vertebrate embryo may crucially depend upon cellular interactions occurring in anterior regions of the embryo. □

Methods

Zebrafish embryos were collected and staged as described²¹. We use the term mid-gastrula to denote the 70%–75% epiboly stage. To ablate ectodermal cells, embryos were mounted in 3% methyl cellulose in embryo medium²¹ and viewed on a fixed-stage Nikon Optiphot microscope; cells were removed by suction using a glass micropipette mounted on a hydrolic micromanipulator and attached to a 10 µl Hamilton syringe. For control ablations, cells from rows 2–5 were ablated or the cells removed from row 1 were placed back in their original positions. For fate-mapping, cells were labelled with diI dissolved in 100% ethanol or were individually injected iontophoretically with a mixture of fluorescent and biotinylated dextrans. For transplantations, donor embryos were injected with a mixture of fluorescent and biotinylated dextrans, and cells transplanted into host embryos were identified using a Vectastain kit to reveal biotin²². All subsequent antibody and *in situ* hybridization protocols followed standard procedures¹¹. For sectioning, embryos were embedded in methacrylate JB4 resin and cut at 7–10 µm on a Leica Ultracut microtome. *hgg1* was isolated by K. A. Barth in a random screen for developmentally expressed complementary DNAs.

Received 23 October; accepted 5 December 1997.

- Lemaire, P. & Kodjabachian, L. The vertebrate organizer: structure and molecules. *Trends Genet* **12**, 525–531 (1996).
- Sasai, Y. & DeRobertis, E. M. Ectodermal patterning in vertebrate embryos. *Dev. Biol.* **182**, 5–20 (1997).
- Woo, K. & Fraser, S. E. Specification of the zebrafish nervous system by nonaxial signals. *Science* **277**, 254–257 (1997).
- Li, Y., Allende, M. L., Finkelstein, R. & Weinberg, E. S. Expression of two zebrafish orthodenticle-related genes in the embryonic brain. *Mech. Dev.* **48**, 229–244 (1994).
- Neave, B., Rodaway, A., Wilson, S. W., Patient, R. & Holder, N. Expression of zebrafish GATA3 (*gta3*) during gastrulation and neurulation suggests a role in the specification of cell fate. *Mech. Dev.* **51**, 169–182 (1995).
- Brand, M. *et al.* Mutations affecting development of the midline and general body shape during zebrafish embryogenesis. *Development* **123**, 129–142 (1996).
- Thisse, C., Thisse, B., Halpern, M. E. & Postlethwait, J. H. Goosecoid expression in neuroectoderm and mesoderm is disrupted in cyclops gastrulas. *Dev. Biol.* **164**, 420–429 (1994).
- Morita, T., Nitta, H., Kiyama, Y., Mori, H. & Mishina, M. Differential expression of two zebrafish *emx* homeoprotein mRNAs in the developing brain. *Neurosci. Lett.* **198**, 131–134 (1995).
- Akimenko, M.-A., Ekker, M., Wegner, J., Lin, W. & Westerfield, M. Combinatorial expression of three zebrafish genes related to *Distal-less*: part of a homeobox gene code for the head. *J. Neurosci.* **14**, 3475–3486 (1994).
- Krauss, S., Concordet, J.-P. & Ingham, P. A functionally conserved homolog of the *Drosophila* segment polarity gene *hh* is expressed in tissues with polarizing activity in zebrafish embryos. *Cell* **75**, 1431–1444 (1993).
- Macdonald, R. *et al.* Regulatory gene expression boundaries demarcate sites of neuronal differentiation in the zebrafish forebrain. *Neuron* **13**, 1039–1053 (1994).
- Barth, K. A. & Wilson, S. W. Expression of zebrafish *nk2.2* is influenced by sonic hedgehog/vertebrate hedgehog-1 and demarcates a zone of neuronal differentiation in the embryonic forebrain. *Development* **121**, 1755–1768 (1995).
- Allende, M. L. & Weinberg, E. The expression pattern of two zebrafish *acheate-scute* homologue (*ash*) genes is altered in the embryonic brain of the *cyclops* mutant. *Dev. Biol.* **166**, 509–530 (1994).
- Shimamura, K. & Rubenstein, J. L. R. Inductive interactions direct early regionalisation of the mouse forebrain. *Development* **124**, 2709–2718 (1997).
- Fürthauer, M., Thisse, C. & Thisse, B. A role for FGF in the dorsoventral patterning of the zebrafish gastrula. *Development* **124**, 4253–4264 (1997).
- Thomas, P. & Beddington, R. Anterior primitive endoderm may be responsible for patterning the anterior neural plate in the mouse embryo. *Curr. Biol.* **6**, 1487–1496 (1996).
- Varlet, L., Collingnon, J. & Robertson, E. J. *nodal* expression in the primitive endoderm is required for specification of the anterior axis during mouse gastrulation. *Development* **124**, 1033–1044 (1997).
- Bouwmeester, T., Kim, S.-H., Sasai, Y., Lui, B. & DeRobertis, E. M. Cerberus is a head-inducing secreted factor expressed in the anterior endoderm of Spemann's organizer. *Nature* **382**, 595–601 (1996).
- Bradley, L., Wainstock, D. & Sive, H. Positive and negative signals modulate formation of the *Xenopus* cement gland. *Development* **122**, 2739–2750 (1996).

- Mizuno, T., Yamaha, E., Wakahara, M., Kuroiwa, A. & Takeda, H. Mesoderm induction in zebrafish. *Nature* **383**, 131–132 (1996).
- Westerfield, M. *The Zebrafish Book* (Univ. Oregon Press, 1996).
- Heisenberg, C. P. *et al.* Genes involved in forebrain development in the zebrafish, *Danio rerio*. *Development* **123**, 191–203 (1996).

Acknowledgements. We thank N. Holder, C. Kimmel, K. Whitlock and Z. Varga for comments on the manuscript and our colleagues for advice throughout this study. We thank many colleagues for providing antibodies and probes. The study was supported by grants from the BBSRC and Wellcome Trust (to S.W.W.) and from the NIH, NATO and W. M. Keck Foundation to M.W. C.H. received a Fellowship from the EC and is currently supported by the BBSRC. S.W. is a Wellcome Trust Senior Research Fellow.

Correspondence and requests for materials should be addressed to C.H. (e-mail: vcgacor@ucl.ac.uk).

Staufen-dependent localization of *prospero* mRNA contributes to neuroblast daughter-cell fate

Julie Broadus*, Sal Fuerstenberg* & Chris Q. Doe

Department of Cell & Structural Biology, Howard Hughes Medical Institute, University of Illinois, Urbana, Illinois 61801, USA

The generation of cellular diversity is essential in embryogenesis, especially in the central nervous system. During neurogenesis, cell interactions or asymmetric protein localization during mitosis can generate daughter cells with different fates^{1–4}. Here we describe the asymmetric localization of a messenger RNA and an RNA-binding protein that creates molecular and developmental differences between *Drosophila* neural precursors (neuroblasts) and their daughter cells, ganglion mother cells (GMCs). The *prospero* (*pros*) mRNA and the RNA-binding protein Staufen (Stau) are asymmetrically localized in mitotic neuroblasts and are specifically partitioned into the GMC, as is Pros protein^{5–7}. Stau is required for localization of *pros* RNA but not of Pros protein. Loss of localization of Stau or of *pros* RNA alters GMC development, but only in embryos with reduced levels of Pros protein, suggesting that *pros* RNA and Pros protein act redundantly to specify GMC fate. We also find that GMCs do not transcribe the *pros* gene, showing that inheritance of *pros* RNA and/or Pros protein from the neuroblast is essential for GMC specification.

The *Drosophila* central nervous system (CNS) develops from stem-cell-like precursors called neuroblasts. Smaller daughter cells (GMCs) 'bud off' from the basal side of the neuroblasts; most GMCs then produce two postmitotic neurons. An important regulator of GMC development is the homeodomain protein Pros. Pros localizes to the apical cytoplasm of neuroblasts at late interphase⁷; at mitosis, it is translocated to the basal cortex where it forms a membrane-associated crescent, and it is subsequently inherited by the GMC in which Pros translocates into the nucleus^{5–7}. Asymmetric cortical localization of Pros is believed to keep Pros protein out of the neuroblast nucleus, and to rapidly generate nuclear Pros protein in the newborn GMC, where Pros establishes GMC-specific gene expression^{8,9}.

Here we describe the cell-cycle-specific asymmetric localization of *pros* mRNA in neuroblasts, which results in its selective partitioning into the daughter GMC. During interphase, most *pros* RNA is localized to the apical side of the neuroblast, where it is found either in the cytoplasm or associated with the cortex (Fig. 1a, Table 1). During mitosis, *pros* RNA is asymmetrically localized to the opposite side of the neuroblast in a basal cortical crescent (Fig. 1a; Table 1). At cytokinesis, *pros* RNA is specifically segregated into the GMC. Localization of *pros* RNA does not reflect a general

*These authors contributed equally to this work.

movement of poly(A⁺) RNA, as a different transcript (*seven-up*) is not localized at any phase of the neuroblast cell cycle (results not shown). Asymmetric cortical crescents of *pros* RNA can also be observed in mitotic sensory organ precursors and adult midgut precursors (results not shown).

The asymmetric localization of *pros* RNA suggests that one or more RNA-binding proteins may also be differentially segregated during neuroblast division. A good candidate for such a protein is the RNA-binding protein Stau, which is asymmetrically localized in the oocyte, is required for localization of *bicoid* and *oskar* RNA, and is detected in the embryonic CNS^{10,11}. We find that Stau shows cell-cycle-specific asymmetric localization in neuroblasts in a pattern that precisely matches the pattern of localization of *pros* RNA and Pros protein (Fig. 2). In late interphase, Stau is localized to the apical cytoplasm or cortex (Fig. 2a). From metaphase through to telophase, Stau is asymmetrically localized as a basal crescent, and segregates into the daughter GMC (Fig. 2b–e). A recent report¹² did not detect basal localization of Stau in neuroblasts, but we observed basal localization of Stau both *in vivo* and *in vitro*¹³, with two different antibodies, and this is consistent with a role for Stau in the basal localization of *pros* RNA (see below). Although Stau and Pros proteins are precisely co-localized in mitotic neuroblasts (Fig. 2f)¹³,

Stau protein localization is normal in *pros* null embryos (Fig. 2g), and Pros protein localization is normal in *stau* null embryos (Fig. 2h). Thus, Stau and Pros proteins are independently localized to the same region, probably by binding to a common anchoring protein.

To determine whether the localization of Stau and *pros* RNA in neuroblasts is microtubule-dependent, as is the localization of Stau and *bicoid* RNA in precellular embryos¹⁰, we depolymerized microtubules with colcemid, arresting neuroblasts in metaphase. Basal crescents of *pros* RNA (Fig. 1b) and Stau protein¹³ were easily observed, and the percentage of *pros* RNA crescents increased from 7% to 63% (*n* = 80) during colcemid treatment, indicating that new *pros* RNA crescents can form in the absence of microtubules. In contrast, actin microfilaments are absolutely required for anchoring Stau to the basal cortex¹³. Localization of Stau and RNA in neuroblasts could occur by diffusion and microfilament-based anchoring.

To determine whether Stau is required for localization of *pros* RNA in neuroblasts, we scored embryos (referred to as *stau* embryos) produced by homozygous *stau*^{D3} flies. These embryos lack both maternal and zygotic Stau. In mitotic neuroblasts of *stau* embryos, basal *pros* RNA localization is reduced from 71% to 27% (Table 1); apical RNA localization is reduced from 56% to 7% in

Table 1 Loss of *stau* reduces asymmetric localization of *pros* RNA

	Neuroblast cell-cycle phase	Subcellular distribution of <i>pros</i> RNA			
		Apical crescent	Basal crescent	Random crescent	Uniform cortical/cytoplasmic location
Wild type (<i>n</i> = 99)	Mitosis	0 (0%)	70 (71%)	1 (1%)	28 (28%)
<i>Stau</i> ⁻ (<i>n</i> = 91)		4 (4%)	25 (27%)	6 (7%)	56 (61%)
Wild type (<i>n</i> = 314)	Interphase	176 (56%)	1 (0%)	0 (0%)	137 (44%)
<i>Stau</i> ⁻ (<i>n</i> = 241)		18 (7%)	6 (2%)	8 (3%)	209 (87%)

* Wild-type embryos are CyO/CyO or *stau*^{D3}/CyO embryos; *stau*⁻ embryos are *stau*^{D3}/*stau*^{D3} embryos from *stau*^{D3}/*stau*^{D3} parents.

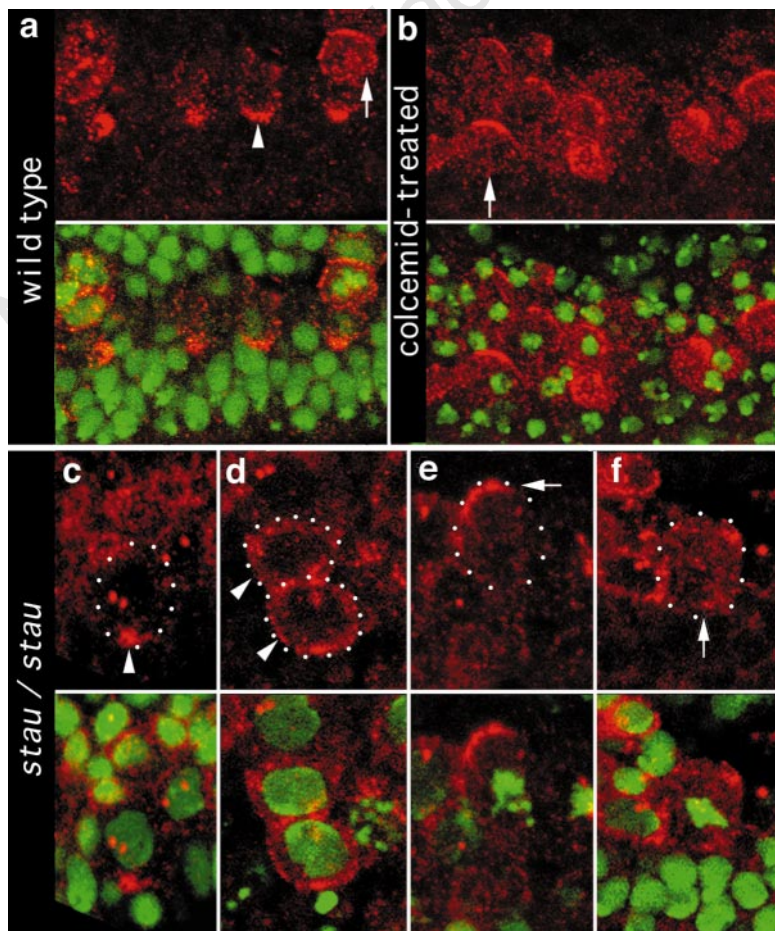


Figure 1 Asymmetric localization of *pros* RNA in neuroblasts requires Stau but not microtubules. Neuroblasts in stage 9–11 embryos were stained for *pros* RNA (red) and DNA (green). The bottom panels show results of double-labelling. Apical side is down; basal side is up. **a**, Wild-type embryo. Interphase neuroblasts have apical *pros* RNA (arrowhead); mitotic neuroblasts have basal cortical *pros* RNA (arrow). **b**, Colcemid-treated embryo. Neuroblasts lack microtubules yet show robust basal crescents of *pros* RNA (arrow). **c–f**, *stau* mutant embryos. **c, d**, Interphase neuroblasts with apical (**c**) or delocalized (**d**) *pros* RNA (arrowheads). **e, f**, Metaphase neuroblasts with basal (**e**) or delocalized (**f**) *pros* RNA (arrows).

interphase neuroblasts (Table 1). Most *stau*⁻ neuroblasts show uniform cytoplasmic or cortical *pros* RNA localization (Fig. 1). Similar results are seen in embryos lacking only zygotic *stau* expression (results not shown). It seems likely that apical Stau protein is required for apical *pros* RNA localization at interphase, and that basal Stau protein is required for basal *pros* RNA localization at metaphase (Fig. 1), however, suggesting that Stau is not the only factor that is able to localize *pros* RNA at the cortex. We conclude that the RNA-binding protein Stau is required for reliable apical and basal localization of *pros* RNA in neuroblasts.

What is the function of the asymmetric segregation of *pros* RNA

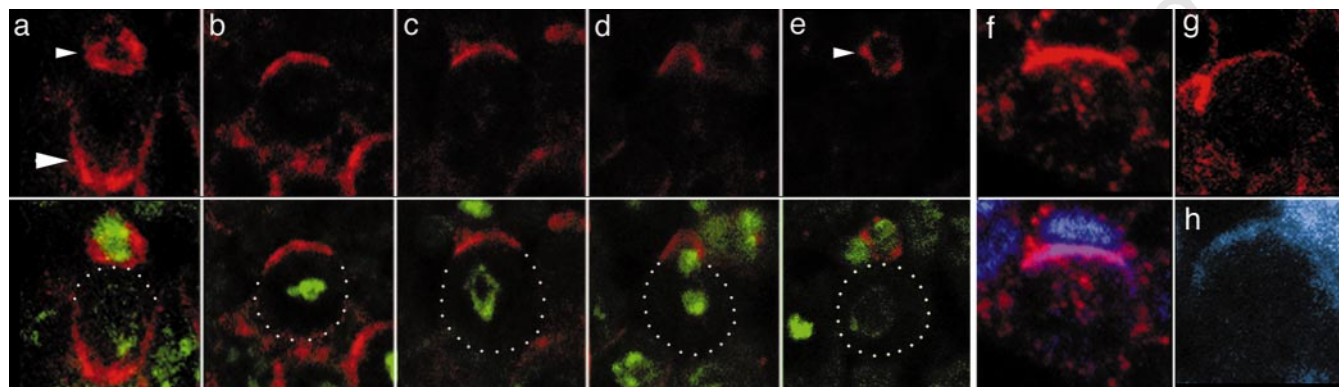


Figure 2 Asymmetric localization of Stau and Pros proteins in neuroblasts. **a–e**, Cell-cycle-specific localization of Stau protein (red) and *stau* DNA (green) in wild-type neuroblasts (bottom panels show results of double-labelling). Apical side is down; basal side is up. **a**, Interphase neuroblast with apically located Stau (large arrowhead; localization of Stau in the GMC cytoplasm is indicated by the small arrowhead). **b**, metaphase, **c**, anaphase and **d**, telophase neuroblasts with Stau

into GMCs? Hybridization with a *pros* intron probe shows that *pros* is transcribed in 67% of neuroblasts ($n = 144$; Fig. 3a), but is transcribed in only 2% of GMCs ($n = 851$; Fig. 3b). Thus, detection of *pros* RNA in GMCs^{7,9,14} (Fig. 3 insets) must reflect inheritance of *pros* RNA from the neuroblast. As GMCs clearly require *pros* function^{8,9}, but do not transcribe the *pros* gene, inheritance of *pros* RNA and/or Pros protein from the neuroblast is essential for GMC specification.

Loss of *pros* RNA localization—but not of Pros protein localization—in *stau* embryos does not alter GMC fate as judged by expression of the markers *even-skipped* (*eve*) or *fushi tarazu* (results not shown). To determine whether localized *pros* RNA and localized

localized to the basal cortex. **e**, Stau is segregated into the GMC where it is cytoplasmic (arrowhead). **f**, Stau (red; top) and Pros (blue; bottom, merged with Stau image) proteins are co-localized at mitosis. **g**, Stau is localized normally in *pros*⁻ mitotic neuroblasts. **h**, Pros is localized normally in *stau*⁻ mitotic neuroblasts.

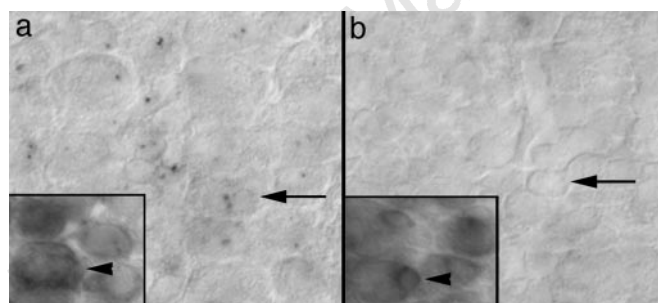


Figure 3 *pros* is transcribed in neuroblasts but not GMCs. A stage-10 embryo was labelled with a *pros* intron probe (**a**, **b**) or a *pros* complementary DNA probe (insets). **a**, Ventral view of the neuroblast layer. Most neuroblasts (arrow) show two chromosomal sites of *pros* transcription; not all sites of transcription are in focus. **b**, Ventral view of the adjacent GMC layer in the same embryo. GMCs (arrow) rarely show *pros* transcription; in this focal plane, none of the GMCs are transcribing *pros*. Insets: a *pros* cDNA probe shows high levels of *pros* RNA (arrowheads) in both neuroblasts and GMCs.

Table 2 Loss of Stau enhances a hypomorphic *pros* GMC phenotype

	Medial Eve ⁺ cells per embryo (n)		
	<i>pros</i> ^{c82}	<i>pros</i> ^{ss214}	<i>pros</i> ^{b149}
Stau ⁺	22.9 ± 4.7 (16)	26.2 ± 7.2 (16)	15.2 ± 6.5 (11)
Stau ⁻ (<i>stau</i> ^{D3})	10.1 ± 3.7 (7)	8.5 ± 4.6 (8)	6.3 ± 3.9 (6)
Stau ⁻ (<i>stau</i> ^{Y9})	6.3 ± 3.4 (3)	8.6 ± 2.4 (5)	n.a.

Segments A1–A7 were scored; the Eve⁺ phenotypes originate in GMCs (embryonic stage 10–11), but we scored neurons (stage 15–16) because the pattern is more reproducible. Medial Eve⁺ cells are defined as all Eve⁺ cells except for those cells of the lateral EL cluster²¹. Wild-type and homozygous *stau*^{D3} or *stau*^{Y9} embryos have ~112 medial Eve⁺ cells; *pros*-null embryos have ~2 medial Eve⁺ cells. n.a., not assayed.

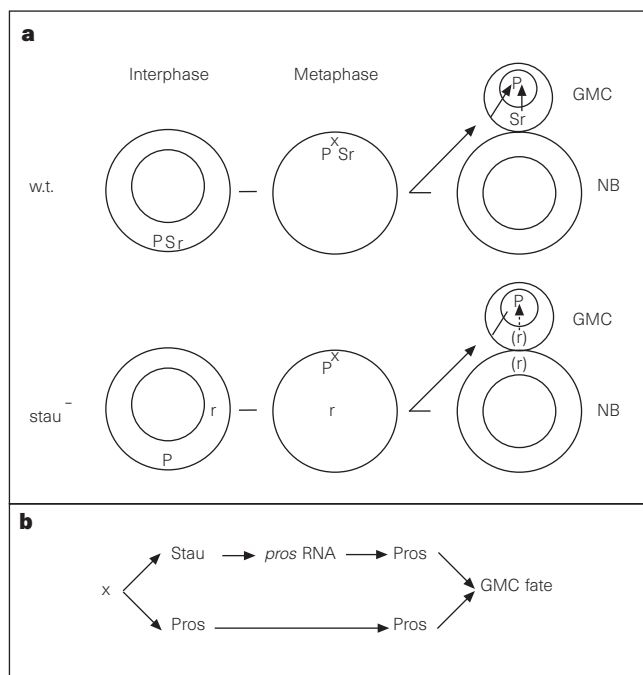


Figure 4 Localization and function of Stau and *pros* RNA in neuroblasts. **a**, Protein and RNA localization in wild-type and *stau* mutant neuroblasts. P, Pros protein; S, Stau protein; r, *pros* RNA; (r), lower level of *pros* RNA; X, putative Pros- and Stau-binding protein; NB, neuroblast. Apical, down; basal, up. **b**, Basal localization pathway: Stau/*pros* RNA and Pros protein are independently localized, perhaps by a common protein (X), and may act redundantly to provide levels of Pros that are necessary to establish GMC-specific gene expression.

Pros protein have redundant functions in GMC development, we used three hypomorphic (weakly active) alleles of *pros* (see Methods) to generate an 'intermediate' GMC phenotype: a reduction in medial Eve⁺ GMCs or their neuronal progeny. We then asked whether loss of *pros* RNA localization could enhance this phenotype. We found that hypomorphic *pros* embryos lacking Stau had less than half the number of medial Eve⁺ cells compared with hypomorphic *pros* embryos (Table 2). This enhancement is observed with two independent *stau* mutations in combination with three different *pros* alleles. These results indicate that *pros* RNA and Pros protein may act redundantly to establish GMC-specific patterns of gene expression (Fig. 4b). However, we cannot rule out the interesting possibility that delocalization of other RNA cargoes of Stau could contribute to the enhancement of the *pros* Eve phenotype.

Our results highlight a mechanism for reliably establishing neuroblast/GMC sibling fates, involving the coordinated but independent partitioning of *pros* RNA and protein into the GMC, where they may act redundantly to establish GMC-specific gene expression. Similarly, ASH1 RNA and Ash1p protein are co-localized and necessary to distinguish mother/daughter-cell fates in yeast¹⁵⁻¹⁷. It remains to be seen whether the asymmetric co-localization of an mRNA and its protein product is a widely used mechanism for reliably establishing distinct daughter-cell fates.

Note added in proof: The newly discovered Miranda protein^{22,23} is likely to be protein X in Fig. 4. □

Methods

*stau*¹⁹, *stau*^{D3} and *pros*¹⁷ are null alleles^{8,11}, *pros*^{B149}, *pros*^{SS214}, and *pros*^{C82} produce decreased Pros-protein levels but normal Pros localization (C.-Y. Peng, J. B. Skeath and C.Q.D., observations). Permeabilized embryos at 4–5 h (ref. 18) were treated with 5 mg ml⁻¹ colcemid (Sigma) for 2 h at 25 °C. Antibody staining was performed using standard methods^{7,19} using mouse anti-Pros⁷, rabbit anti-Stau¹¹, and rat anti-Stau (S.F. and C.Q.D., results not shown). RNA *in situ* hybridization was performed as described previously²⁰; fluorescent detection was done with 1:200 fluorescein-isothiocyanate-conjugated anti-digoxigenin (Boehringer) with propidium iodide or sonicated phenylenediamine¹⁹ for DNA detection. Cell-cycle staging was based on DNA condensation and segregation. Detailed methods are available on request.

Received 27 May; accepted 17 November 1997.

1. McConnell, S. K. Constructing the cerebral cortex: neurogenesis and fate determination. *Neuron* **15**, 761–768 (1995).
2. Guenther, C. & Garriga, G. Asymmetric distribution of the *C. elegans* HAM-1 protein in neuroblasts enables daughter cells to adopt distinct fates. *Development* **122**, 3509–3518 (1996).
3. Jan, Y. N. & Jan, L. Y. Maggot's hair and bug's eye: role of cell interactions and intrinsic factors in cell fate specification. *Neuron* **14**, 1–5 (1995).
4. Lin, H. & Schagat, T. Neuroblasts: a model for the asymmetric division of stem cells. *Trends Genet.* **13**, 33–39 (1996).
5. Hirata, J., Nakagoshi, H., Nabeshima, Y. & Matsuzaki, F. Asymmetric segregation of the homeodomain protein Prospero during *Drosophila* development. *Nature* **377**, 627–630 (1995).
6. Knoblich, J. A., Jan, L. Y. & Jan, Y. N. Asymmetric segregation of Numb and Prospero during cell division. *Nature* **377**, 624–627 (1995).
7. Spana, E. & Doe, C. Q. The prospero transcription factor is asymmetrically localized to the cell cortex during neuroblast mitosis in *Drosophila*. *Development* **121**, 3187–3195 (1995).
8. Doe, C. Q., Chu-LaGriff, Q., Wright, D. M. & Scott, M. P. The *prospero* gene specifies cell fates in the *Drosophila* central nervous system. *Cell* **65**, 451–464 (1991).
9. Vaessin, H. *et al.* prospero is expressed in neuronal precursors and encodes a nuclear protein that is involved in the control of axonal outgrowth in *Drosophila*. *Cell* **67**, 941–953 (1991).
10. Ferrandon, D., Elphick, L., Nüsslein-Volhard, C. & St Johnston, D. Staufin protein associates with the 3' UTR of *bicoid* mRNA to form particles that move in a microtubule-dependent manner. *Cell* **79**, 1221–1232 (1994).
11. St Johnston, D., Beuchle, D. & Nüsslein-Volhard, C. *staufer*, a gene required to localize maternal RNA in the *Drosophila* egg. *Cell* **66**, 51–63 (1991).
12. Li, P., Yang, X., Wasser, M., Cai, Y. & Chia, W. Inscuteable and Staufin mediate asymmetric localization and segregation of prospero RNA during *Drosophila* neuroblast cell divisions. *Cell* **90**, 437–447 (1997).
13. Broadus, J. & Doe, C. Q. Extrinsic cues, intrinsic cues, and microfilaments regulate asymmetric protein localization in *Drosophila* neuroblasts. *Curr. Biol.* **7**, 827–835 (1997).
14. Matsuzaki, F., Koizumi, K., Hama, C., Yoshioka, T. & Nabeshima, Y. Cloning of the *Drosophila prospero* gene and its expression in ganglion mother cells. *Biochem. Biophys. Res. Commun.* **182**, 1326–1332 (1992).
15. Long, R. M. *et al.* Mating type switching in yeast controlled by asymmetric localization of ASH1 mRNA. *Science* **277**, 383–387 (1997).
16. Takizawa, P. A., Sil, A., Swedlow, J. R., Herskowitz, I. & Vale, R. D. Actin-dependent localization of an RNA encoding a cell-fate determinant in yeast. *Nature* **389**, 90–93 (1997).
17. Bobola, N., Jansen, R.-P., Shin, T. & Nasmyth, K. Asymmetric accumulation of Ash1p in postanaphase nuclei depends on a myosin and restricts yeast mating-type switching to mother cells. *Cell* **84**, 699–709 (1996).

18. Bodmer, R., Carretto, R. & Jan, Y. N. Neurogenesis of the peripheral nervous system in *Drosophila* embryos: DNA replication patterns and cell lineages. *Neuron* **3**, 21–32 (1989).
19. Lundell, M. J. & Hirsch, J. A new visible light fluorochrome for confocal microscopy. *Biotechniques* **16**, 434–440 (1994).
20. Broadus, J. B. & Doe, C. Q. Evolution of neuroblast identity: *seven-up* and *prospero* expression reveal homologous and divergent cell fates in *Drosophila* and *Schistocerca*. *Development* **121**, 3989–3996 (1995).
21. Patel, N. H., Schafer, B., Goodman, C. S. & Holmgren, R. The role of segment polarity genes during *Drosophila* neurogenesis. *Genes Dev.* **3**, 890–904 (1989).
22. Shen, C.-P., Jan, L. Y. & Jan, Y. N. Miranda is required for the asymmetric localization of Prospero during mitosis in *Drosophila*. *Cell* **90**, 449–458 (1997).
23. Ikeshima-Kataoka, H., Skeath, J. B., Nabeshima, Y., Doe, C. Q. & Matsuzaki, F. Miranda directs Prospero to a daughter cell during *Drosophila* asymmetric divisions. *Nature* **390**, 625–629 (1997).

Acknowledgements. We thank C.-Y. Peng for help with genetics; C.-Y. Peng, F. Matsuzaki and B. Chia for sharing unpublished results; D. St Johnston for Stau antiserum; E. Spana for *pros* intron DNA; and C. Thummel and F. Gertler for comments. This work was supported by an NIH postdoctoral fellowship to S.F. and by the HHMI, of which C.Q.D. is an associate investigator.

Correspondence and requests for materials should be addressed to C.Q.D.

HLA-E binds to natural killer cell receptors CD94/NKG2A, B and C

Veronique M. Braud*†, David S. J. Allan*†, Christopher A. O'Callaghan*, Kalle Söderström‡, Annalisa D'Andrea‡, Graham S. Ogg*, Sasha Lazetic‡, Neil T. Young§, John I. Bell*, Joseph H. Phillips‡, Lewis L. Lanier‡ & Andrew J. McMichael*

* Institute of Molecular Medicine, John Radcliffe Hospital, Oxford OX3 9DS, UK
 † Department of Immunology, DNAX Research Institute of Molecular and Cellular Biology, Palo Alto, California 94304, USA
 ‡ Nuffield Department of Surgery, John Radcliffe Hospital, Oxford OX3 9DU, UK
 † These authors contributed equally to this work.

The protein HLA-E is a non-classical major histocompatibility complex (MHC) molecule of limited sequence variability. Its expression on the cell surface is regulated by the binding of peptides derived from the signal sequence of some other MHC class I molecules^{1,2}. Here we report the identification of ligands for HLA-E. We constructed tetramers³ in which recombinant HLA-E and β2-microglobulin were refolded with an MHC leader-sequence peptide, biotinylated, and conjugated to phycoerythrin-labelled Extravidin. This HLA-E tetramer bound to natural killer (NK) cells and a small subset of T cells from peripheral blood. On transfectants, the tetramer bound to the CD94/NKG2A, CD94/NKG2B and CD94/NKG2C NK cell receptors, but did not bind to the immunoglobulin family of NK cell receptors (KIR). Surface expression of HLA-E was enough to protect target cells from lysis by CD94/NKG2A⁺ NK-cell clones. A subset of HLA class I alleles has been shown to inhibit killing by CD94/NKG2A⁺ NK-cell clones⁴⁻⁶. Only the HLA alleles that possess a leader peptide capable of upregulating HLA-E surface expression confer resistance to NK-cell-mediated lysis, implying that their action is mediated by HLA-E, the predominant ligand for the NK cell inhibitory receptor CD94/NKG2A.

The non-classical MHC class Ib molecule HLA-E has a broad tissue distribution⁷. Like its homologue, the mouse MHC class Ib Qa-1⁸⁻¹¹, HLA-E preferably binds to a peptide derived from amino-acid residues 3–11 of the signal sequences of most HLA-A, -B, -C, and -G molecules, but cannot bind its own leader peptide^{1,2}. Cell-surface expression of HLA-E depends on a functional transporter associated with antigen processing (TAP), and is upregulated by the binding of the peptides derived from MHC molecule signal sequences². The close correlation between the surface expression of HLA-E and of certain other MHC class I molecules suggested a possible role for HLA-E in NK-cell-mediated recognition of target cells.

To test this hypothesis, we constructed tetrameric complexes